Hindawi
Journal of Nanomaterials
Volume 2019, Article ID 5106909, 9 pages
https://doi.org/10.1155/2019/5106909

Research Article

Effective Approach for an Order-of-Magnitude-Accurate Evaluation of the Electron Mobility in Colloidal Quantum Dot Films

Francisco M. Gómez-Campos,[1,2] Salvador Rodríguez-Bolívar,[1,2] and Marco Califano[3]

[1]*Departamento de Electrónica y Tecnología de Computadores, Facultad de Ciencias, Universidad de Granada, 18071 Granada, Spain*
[2]*CITIC-UGR, C/Periodista Rafael Gómez Montero, n 2, Granada, Spain*
[3]*Pollard Institute, School of Electronic and Electrical Engineering, University of Leeds, Leeds LS2 9JT, UK*

Correspondence should be addressed to Marco Califano; m.califano@leeds.ac.uk

Received 16 May 2018; Revised 29 October 2018; Accepted 1 November 2018; Published 24 February 2019

Academic Editor: Peter Reiss

Being able to estimate the electron mobility of colloidal quantum dot films is of great importance for determining their suitability to specific applications and would lead to huge savings in terms of time and resources that may otherwise be wasted trying to build and optimize a device whose transport characteristics can be predicted to be poor from the outset. This task is however complicated by the complexity of the system and the large number of parameters that can potentially affect the final result. Here, we derive a simple, fitting-parameter-free, order-of-magnitude-accurate expression to estimate the dark mobility of such 2D structures and validate it by applying it to real systems and comparing its predictions with those of other recently proposed approaches and with available experimental data. The results quantify the superiority of our expression to estimate mobilities in colloidal quantum dot films.

1. Introduction

The use of semiconductor colloidal quantum dots (CQDs) as building blocks for optoelectronic and energy-harvesting devices has become widespread [1–5]. Such applications usually require these nanostructures to be arrayed in 2D or 3D supercrystals, whose optical properties retain similar characteristics (i.e., optical gap) to their constituents. The transport properties of these arrays, on the other hand, cannot be as easily inferred from those of the single dots in solution. In this respect, the evaluation of the film mobility is of particular interest, as its magnitude determines the range of applications the material would be better suited for [1, 2, 6–8]. Given the complexity of the system, however, such an evaluation is not trivial. A simple expression for estimating the maximum dark mobility in 3D CQD supercrystals, obtained within the k·p framework under the assumption that fluctuations in the size of the CQDs represent the main source of electron scattering, was proposed recently by Shabaev et al. [9]. Here, we derive, under the same assumptions, an alternative expression for quantum dot films suitable for atomistic approaches which does not make use of any fitting parameter (the only unknown parameter being represented by the density of defects in the array) but only relies on the calculated band structure of the film and of its constituents. When compared with available experimental data and the results of the expression proposed by Shabaev et al., our expression reveals a superior accuracy and predicting power. In particular, for arrays of CdSe and PbSe CQDs, our predicted mobilities are consistent with those observed experimentally in these systems [7, 10], whereas the mobility values obtained using the expression from Ref. [9] are at least one order of magnitude smaller than our estimates and over a factor of 20 smaller than the experiment.

2. Method

2.1. The Wave Functions. We consider a 2D array of quantum dots perfectly ordered in space. In order to solve the Schrödinger equation for the system, we implement a

tight-binding approach, where the wave functions of the periodic system are described as linear combinations of isolated quantum dot wave functions [9, 11], obtained here within the framework of the atomistic semiempirical pseudopotential method [12]:

$$\psi(\vec{r}) = \sum_{m,\vec{R}_n} b_m\left(\vec{R}_n\right)\phi_m\left(\vec{r} - \vec{R}_n\right), \tag{1}$$

where m indicates a particular state of the isolated quantum dot and $\vec{R}_n$ is the position of each quantum dot in the array.

Although the standard tight-binding (T-B) approach, traditionally employed in the modelling of semiconductor bulk solids [13, 14], and its main equations are well known in the case of the bulk, it is nevertheless instructive to show their detailed derivation in the case of a 2D array of CQDs, as is discussing the assumptions that lead to the different approximations and simplifications. In this spirit, we will therefore follow a more didactic route to obtain our expression for the electron dark mobility (most of Section 2.1 is standard T-B [14] and can be skipped by the experienced reader. The main result, its limits of applicability, and the approximations used are discussed in detail in Sections 2.2 and 2.3).

According to Bloch's theorem, the following relationship holds between the coefficients $b_m(\vec{R}_n)$ and those at $\vec{R}_n = 0$, $b_m(0)$:

$$b_m\left(\vec{R}_n\right) = e^{j\vec{q}\cdot\vec{R}_n} b_m(0), \tag{2}$$

where $\vec{q}$ is a vector in reciprocal space. Therefore, the knowledge of the coefficients for the reference quantum dot (the one at the origin of coordinates) is sufficient to describe the whole of the array. Substituting equation (2) into equation (1), we get [14]

$$\psi(\vec{r}) = \sum_{m,\vec{R}_n} e^{j\vec{q}\cdot\vec{R}_n} b_m(0)\phi_m\left(\vec{r} - \vec{R}_n\right). \tag{3}$$

When using equation (3) to solve the Schrödinger equation of the periodic system, we obtain a set of eigenvalues and wave functions for each $\vec{q}$. Such eigenvalues can be grouped into minibands in the same way as in the case of the bulk semiconductor. Therefore, the resulting wave functions depend on $\vec{q}$ and the specific miniband c [14]

$$\psi_{q,c}(\vec{r}) = \sum_{m,\vec{R}_n} e^{j\vec{q}\cdot\vec{R}_n} b_{mqc}\phi_m\left(\vec{r} - \vec{R}_n\right), \tag{4}$$

where, for ease of notation, we have simplified $b_{mqc}(0)$ as b_{mqc}. This expression for the wave function is inserted into the Schrödinger equation, and both sides are left multiplied by $\phi_m(\vec{r})$—the wave functions of the reference quantum dot at the origin—yielding a matrix equation, whose solution provides the eigenenergies and the coefficients b_{mqc}.

The wave function needs now to be renormalized over the entire space, so that it satisfies

$$\int \psi^*_{qc}(\vec{r})\psi_{qc}(\vec{r})\,d\vec{r} = \sum_{m,\vec{R}_n} e^{-j\vec{q}\cdot\vec{R}_n} b^*_{mqc} \sum_{s,\vec{R}_t} e^{j\vec{q}\cdot\vec{R}_t} b_{sqc} \int \phi^*_m\left(\vec{r} - \vec{R}_n\right)\phi_s\left(\vec{r} - \vec{R}_t\right)d\vec{r} = 1. \tag{5}$$

Most of the integrals in equation (5) are negligible, as there is no overlap between the wave functions of dots that are far apart, except when $\vec{R}_t$ and $\vec{R}_n$ are the positions of nearest neighbors. If N is the number of quantum dots, the summation over $\vec{R}_n$ can therefore be replaced by N times the integral for a particular $\vec{R}_n$, e.g., $\vec{R}_n = 0$. This leads to the following simplification:

$$\int \psi^*_{qc}(\vec{r})\psi_{qc}(\vec{r})\,d\vec{r} = N\sum_m\sum_s b^*_{mqc}b_{sqc}\left\{\delta_{m,s} + \sum_{\vec{R}_p\neq 0} e^{j\vec{q}\cdot\vec{R}_p} \int \phi^*_m(\vec{r})\phi_s\left(\vec{r} - \vec{R}_p\right)d\vec{r}\right\} \equiv NK, \tag{6}$$

where $\vec{R}_p$ are the positions of the nearest neighbors of the quantum dot at the origin (the case $\vec{R}_p = 0$ is represented by the term $\delta_{m,s}$), and

$$K \equiv \sum_m\sum_s b^*_{mqc}b_{sqc}\left\{\delta_{m,s} + \sum_{\vec{R}_{p\neq 0}} e^{j\vec{q}\cdot\vec{R}_p} \int \phi^*_m(\vec{r})\phi_s\left(\vec{r} - \vec{R}_p\right)d\vec{r}\right\}. \tag{7}$$

The wave function

$$\tilde{\psi}_{q,c}(\vec{r}) = \sum_{m,\vec{R}_n} e^{j\vec{q}\cdot\vec{R}_n} \tilde{b}_{mqc}\phi_m\left(\vec{r} - \vec{R}_n\right), \tag{8}$$

where

$$\tilde{b}_{mqc} = \frac{b_{mqc}}{\sqrt{NK}} \tag{9}$$

now satisfies

$$\int \tilde{\psi}^*_{qc}(\vec{r})\tilde{\psi}_{qc}(\vec{r})d\vec{r} = N\sum_m\sum_s \tilde{b}^*_{mqc}\tilde{b}_{sqc}\left\{\delta_{m,s} + \sum_{\vec{R}_{p\neq 0}} e^{j\vec{q}\cdot\vec{R}_p}\int \phi^*_m(\vec{r})\phi_s\left(\vec{r}-\vec{R}_p\right)d\vec{r}\right\} = 1. \tag{10}$$

So far, we have followed standard T-B theory [14], although applied to CQD films instead of bulk materials. In the next section, we will introduce some working hypotheses and approximations that will lead to a simplified, but nevertheless, order-of-magnitude-accurate expression to calculate the dark electron mobility in these systems.

2.2. The Scattering Model. The Hamiltonian of the perfectly periodic system is

$$\left[T + \sum_{\vec{R}_n} V_o\left(\vec{r}-\vec{R}_n\right)\right]\tilde{\psi}(\vec{r}) = E\tilde{\psi}(\vec{r}). \tag{11}$$

We introduce a small perturbation by replacing one of the single quantum dot potentials with that of a smaller quantum dot (here, we implicitly make the assumption that, as pointed out recently [9], fluctuations in the size of the CQDs represent the main source of electron scattering)

$$\left[T + \sum_{\vec{R}_n} V_o\left(\vec{r}-\vec{R}_n\right) + \left(V_{\text{other size}}\left(\vec{r}-\vec{R}_{\text{defect}}\right) - V_o\left(\vec{r}-\vec{R}_{\text{defect}}\right)\right)\right]\tilde{\psi}'(\vec{r}) = E'\tilde{\psi}'(\vec{r}). \tag{12}$$

The scattering probability for the transition from state $|i\rangle$ to state $|f\rangle$ due to this perturbation can be obtained using Fermi's golden rule [15]

$$\Gamma_{i\to f} = \frac{2\pi}{\hbar}\sum_f \delta(E_f - E_i)\left|\left\langle\tilde{\psi}_f|\Delta V|\tilde{\psi}_i\right\rangle\right|^2, \tag{13}$$

where $\Delta V = (V_{\text{other size}}(\vec{r}-\vec{R}_{\text{defect}}) - V_o(\vec{r}-\vec{R}_{\text{defect}}))$, and the matrix element can be expressed as

$$\left\langle\tilde{\psi}_f|\Delta V|\tilde{\psi}_i\right\rangle = \sum_{m,\vec{R}_n} e^{-j\vec{q}_f\cdot\vec{R}_n}\tilde{b}^*_{mq_fc_f}\sum_{s,\vec{R}_t} e^{j\vec{q}_i\cdot\vec{R}_t}\tilde{b}_{sq_ic_i}\int\phi^*_m\left(\vec{r}-\vec{R}_n\right)\Delta V\phi_s\left(\vec{r}-\vec{R}_t\right)d\vec{r}. \tag{14}$$

Here, the m and f subindices refer to the final states, while s and i to the initial state.

In equation (14), $\vec{R}_n$ and $\vec{R}_t$ vary throughout the whole system; however, for similar reasons to those discussed above in relation to equation (5), most of the integrals are expected to be negligible except those where $\vec{R}_n = \vec{R}_t = \vec{R}_{\text{defect}}$. Equation (14) can therefore be approximated by

$$\left\langle\tilde{\psi}_f|\Delta V|\tilde{\psi}_i\right\rangle \simeq \sum_{m,s} e^{j\left(\vec{q}_i-\vec{q}_f\right)\cdot\vec{R}_{\text{defect}}}\tilde{b}^*_{mq_fc_f}\tilde{b}_{sq_ic_i}\int\phi^*_m\left(\vec{r}-\vec{R}_{\text{defect}}\right)\Delta V\phi_s\left(\vec{r}-\vec{R}_{\text{defect}}\right)d\vec{r}. \tag{15}$$

If we now set, without loss of generality, $\vec{R}_{\text{defect}} = 0$, the matrix element becomes

$$\left\langle\tilde{\psi}_f|\Delta V|\tilde{\psi}_i\right\rangle \simeq \sum_{m,s}\tilde{b}^*_{mq_fc_f}\tilde{b}_{sq_ic_i}\int\phi^*_m(\vec{r})\Delta V\phi_s(\vec{r})d\vec{r}. \tag{16}$$

As a further approximation, we assume that all the imperfections (i) are exactly the same, (ii) give the same contribution, and (iii) are uncorrelated [14]. Following the convention adopted for ionized impurity scattering in semiconductors [16], which process is formally similar to the scattering mechanism considered here, the scattering rates for a film containing N_{defects} defects are obtained multiplying by N_{defects} the rate calculated for a single defect. We can therefore rewrite equation (13) as eq. (16.14) in [14], where, however, we have substituted the matrix element between the properly normalised wave functions, appropriate for the case of a CQD film:

$$\Gamma_{i\to f} \simeq \frac{2\pi}{\hbar}\sum_f \delta(E_f - E_i)\frac{N_{\text{defects}}}{N^2K_iK_f}\left|\sum_{m,s} b^*_{mq_fc_f}b_{sq_ic_i}\int\phi^*_m(\vec{r})\Delta V(\vec{r})\phi_s(\vec{r})d\vec{r}\right|^2. \tag{17}$$

Finally, we replace $\sum_f\delta(E_f - E_i)$ with $\int\rho(E)\delta(E_f - E)dE$, where $\rho(E)$ is the density of states, obtaining

$$\Gamma_{i\to f} \simeq \frac{2\pi}{\hbar}\rho(E_f)\frac{N_{\text{defects}}}{N^2K_iK_f}\left|\sum_{m,s} b^*_{mq_fc_f}b_{sq_ic_i}\int\phi^*_m(\vec{r})\Delta V(\vec{r})\phi_s(\vec{r})d\vec{r}\right|^2. \tag{18}$$

Around parabolic miniband extrema in a 2D system such as a CQD film, the density of states can be expressed as

$$\rho(E) = \begin{cases}\dfrac{m_{\text{mb}}NA_{\text{uc}}}{2\pi\hbar^2}, & E > 0 \equiv E_{\min}(\text{miniband}),\\ 0, & E < 0 \equiv E_{\min}(\text{miniband}),\end{cases} \tag{19}$$

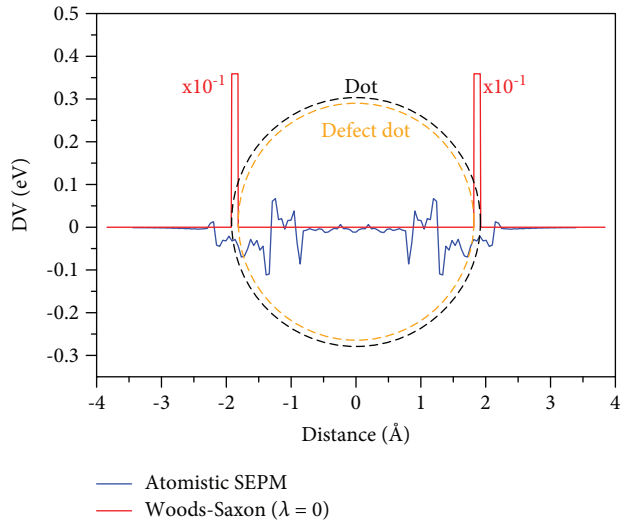

FIGURE 1: Potential difference ΔV according to two different theoretical approaches: atomistic semiempirical pseudopotential method (SEPM, blue line) and the continuum-like k·p method of Ref. [9] (red line). The contours of the two dot sizes they refer to (the "normal" dot, black line, and the "defect" dot, orange line) are also outlined.

where m_{mb} is the miniband effective mass, A_{uc} is the area of the superlattice unit cell, and NA_{uc} is the total area of the system.

The scattering probability therefore becomes

$$\Gamma_{i\to f} \simeq \frac{m_{\mathrm{mb}} A_{\mathrm{uc}}}{\hbar^3} \frac{N_{\mathrm{defects}}}{NK_iK_f} \left| \sum_{m,s} b^*_{mq_fc_f} b_{sq_ic_i} \int \phi^*_m(\vec{r}) \Delta V(\vec{r}) \phi_s(\vec{r}) d\vec{r} \right|^2. \quad (20)$$

A fundamental step in the use of equation (20) is the calculation of the product $\phi^*_m(\vec{r})\Delta V(\vec{r})\phi_s(\vec{r})$: the theoretical framework adopted to compute its factors will crucially determine the accuracy of this expression's predictions. The quantity ΔV can be calculated directly from the single potentials for the two dot sizes. As these potentials nearly coincide over a volume corresponding to the (smaller) defect-dot core, and as they are considered at the same position in space, their difference (ΔV) is negligible everywhere except over the volume of a thin shell enclosing the surface of the larger dot. Within a continuum-like approach, such as the effective mass k·p method of Ref. [9], ΔV is constant and depends only on the depth of the potential well U_0, when the single-dot potentials are square wells (i.e., one assumes $\lambda = 0$ in the Woods-Saxon potential—see red line in Figure 1—as it is done in Ref. [9] in the low-energy case). Therefore, the difference in the magnitude of ΔV in different materials would be equal to the difference in confining potentials U_0. As in Ref. [9] the latter are treated as fitting parameters they are assumed to be the same for different materials. As a consequence, the values of the wave functions in the shell for different materials are also very similar, as, in this approach, they depend on the effective mass and the ground state energy, which, in turn, depends on the confining potential. The difference in scattering rates between identical films of CQDs that differ only in the dot material is therefore determined mainly by the difference in the miniband effective masses. The same is however not true in the case of atomistic methods. We find [17] that the nanoscopic details of the material's atomic potentials (see blue line in Figure 1) and the magnitude and symmetry of the atomistic electron wave functions in this shell-shaped region in space play a crucial role in the determination of the scattering rates and the film mobility, which can differ by orders of magnitude for materials with similar miniband effective masses.

2.3. Mobility in the Lowest Miniband of a CQD Film. Carrier mobility in semiconductors can be roughly estimated using [18]

$$\mu = \frac{e\langle\tau\rangle}{m_{\mathrm{mb}}}, \quad (21)$$

where m_{mb} is the effective mass in the miniband (obtained here by approximating the miniband curvature around the minimum ($q = 0$) with a parabola according to

$$m_i = \frac{\hbar^2 q_i^2}{2(E_i - E_0)}, \quad (22)$$

where $i = x, y$ are two perpendicular in-plane directions, E_i is the calculated energy at $q = q_i$ (for small q_i), E_0 is the energy at $q = 0$ - for an example of our calculated band structure for a film of CdSe CQDs with $D = 3.84$ nm, see Figure 2), e is the electron charge, and $\langle\tau\rangle$ is the average scattering time.

Based on this model, we develop an approach to estimate the mobility in CQD films, valid in the low-energy limit under the assumption that transport occurs within the parabolic part of the spectrum [9]. As in this framework the electrons mainly populate the minimum of the lowest-energy conduction miniband, and since the scattering due to variations in the dot size is elastic, in the calculation of the average scattering time, both initial and final states can be described using the lowest-energy-state wave function. Indeed, the absence of degeneracies around the lowest miniband minima in the electronic structure calculated for a variety of materials and configurations [19] supports the assumption that elastic scattering is an intraminiband process in these systems. This assumption restricts the validity of our calculated mobility to the low-electric field case, where the electron state is not significantly modified by drift.

As the scattering time can be expressed as the inverse of the scattering probability obtained using Fermi's golden rule, the problem of calculating the mobility reduces to that of calculating Γ

$$\mu = \frac{q}{\Gamma m_{\mathrm{mb}}}. \quad (23)$$

Substituting equation (20) into equation (23), we therefore obtain

$$\mu_{OM} = \frac{q}{\left(m_{\mathrm{mb}}^2 A_{\mathrm{uc}}/\hbar^3\right)\left(N_{\mathrm{defects}}/NK_iK_f\right)\left|\sum_{m,s} b^*_{mq_fc_f} b_{sq_ic_i} \int \phi^*_m\left(\vec{r}\right)\Delta V\left(\vec{r}\right)\phi_s\left(\vec{r}\right)d\vec{r}\right|^2} \equiv \frac{\mu^0_{OM}}{\rho_{\mathrm{defects}}}, \quad (24)$$

where $\rho_{\mathrm{defects}} = N_{\mathrm{defects}}/N$, which, importantly, is independent of temperature, consistently with the expected temperature independence of the scattering rate Γ in the case of impurity scattering [18].

Equation (24) is an order-of-magnitude expression for the mobility of an electron in the lowermost miniband of a 2D CQD array, valid for an intraminiband elastic scattering process.

From this expression, using Einstein's relation

$$L_{\mathrm{diff}} = \sqrt{D\tau}, \quad (25)$$

where $D = \mu k_B T/e$, k_B is the Boltzmann constant, T is the temperature, and e the electron charge, an order-of-magnitude estimate for the diffusion length in the system can also be obtained as

$$L^{OM}_{\mathrm{diff}} = \frac{\mu}{e}\sqrt{k_B T m_{\mathrm{mb}}}. \quad (26)$$

3. Results and Discussion

In order to determine its accuracy, we will now employ equation (24) to estimate the mobility in films of CdSe and PbSe CQDs (their electronic structures are calculated using the pseudopotentials from [12] and [20], respectively) and compare its predictions with those of a recently published expression [9] and with experiment. In a recent paper, Shabaev et al. [9] derived, within the framework of the k·p approach, and under the assumption that fluctuations in the size of the CQDs represent the main source of electron scattering, an approximate expression for the dark mobility in a simple cubic 3D supercrystal, which, in the case of touching dots, reduces to

$$\mu_d^{\max} = \frac{2^8}{3\pi^{3/2}}\frac{eR^2}{\hbar}\frac{t^{5/2}}{\chi^2 U_0^2}\frac{1}{\sqrt{k_B T}}. \quad (27)$$

Here, R is the dot radius, t is the overlap integral, χ the size dispersion, U_0 the confining potential for the electrons, T is the temperature, and k_B is the Boltzmann constant.

All quantities (integrals) to be inserted in equations (24) and (27) were calculated using atomistic wave functions obtained within the framework of the semiempirical pseudopotential method [12] (up to 12 single-dot states were included in the calculations of the film's band structure—an example of which is presented in Figure 2 for the case of CdSe CQDs with $D = 3.84$ nm). The results are summarized in Table 1.

As in the calculation of the isolated dot wave functions we take the vacuum level as a reference zero energy, the depth U_0 of the electron well is determined by the absolute value of the calculated position of the conduction band, in the limit of infinitely large dots (which is in good agreement with the asymptotic behavior observed in recent accurate photoelectron spectroscopic measurements [21]).

For arrays of PbSe CQDs with $D = 2.52$ nm, equation (24) predicts very large mobilities, of the order of 65 $\mathrm{cm^2\ V^{-1}s^{-1}}$, consistent with the record-high electron mobilities (10 $\mathrm{cm^2\ V^{-1}s^{-1}}$) measured recently in films of PbSe dots with $D = 6$ nm [7] (whose mobility, given their larger size, is expected to be considerably smaller than that calculated for the dots considered here). The estimate obtained using equation (27), which, for the same reason, is expected to be much larger than that observed for dots with $D = 6$ nm, is instead 0.8 $\mathrm{cm^2\ V^{-1}s^{-1}}$.

In the case of wurtzite CdSe films with the parameters listed in Table 1, equation (24) yields mobilities of 12 $\mathrm{cm^2\ V^{-1}s^{-1}}$, again in good agreement with the dark mobilities (27 $\mathrm{cm^2\ V^{-1}s^{-1}}$) [10] observed experimentally in these systems. In contrast, equation (27) predicts, for the same parameters, a room temperature mobility of 1.27 $\mathrm{cm^2\ V^{-1}s^{-1}}$, an order of magnitude smaller than the estimate obtained using equation (24), and a factor of over 20 smaller than experiment. Indeed, in order to reproduce experiment [10], an electron confining potential of about 0.6 eV (more appropriate for epitaxial dots than colloidal nanocrystals) must be assumed in equation (27) (U_0 is treated as a fitting parameter in Ref. [9]). This is because the continuum-like approach of Ref. [9] largely underestimates the overlap integrals t. Any reduction in the electron confinement leads, in fact, to a substantial increase in the mobilities of equation (27), owing to the combined effect of an increase in the overlap integral t (raised to the power of 5/2 in the numerator of equation (27)) and the decrease of U_0 itself (raised to the power of 2 in the denominator of equation (27)). As an example, a reduction of 0.5 [1.0] eV in U_0 alone (i.e., without considering the corresponding increase in the overlap integral t) would lead to a 35% [92%] increase in the mobility calculated for an array of CdSe dots with $D = 3.8$ nm.

It is also worth noting that, while the mobility in equation (24), together with an inverse dependence on the size difference between nominal-size dots and scatterers also exhibits a crucial inverse dependence on the density of the scattering centers as one would expect (see, e.g., eq. (5.58) in Ref. [18], or eq. (16.14) in Ref. [14]), equation (27) only accounts for the former through the size dispersion χ but lacks any explicit dependence on the latter. As mentioned above, the defects considered here consist of smaller dots, randomly distributed within the array, with a 1% density. This low-density limit ensures the absence of defect clustering in the presence of which the present treatment would no longer be valid. At the same time, this choice makes it easier

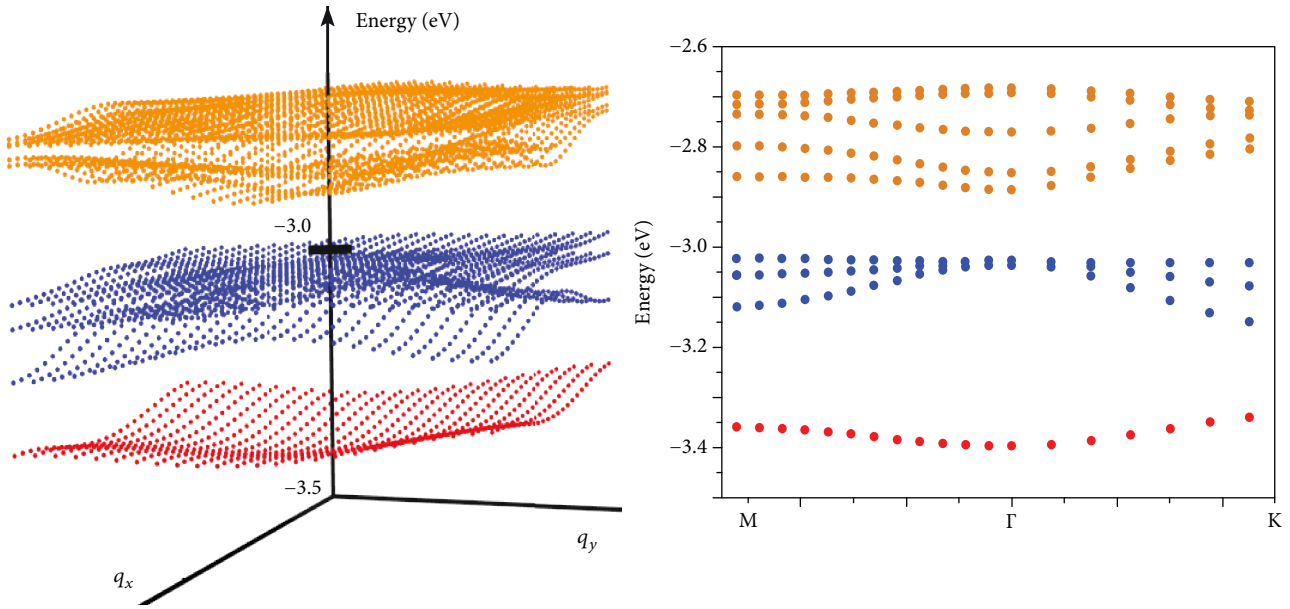

FIGURE 2: Calculated band structure for a 2D array of wurtzite CdSe CQDs with $D = 3.84$ nm, placed 1 bond length apart: the upper panel displays the minibands in 3D; the lower panel presents the traditional 2D representation for the minibands. In both panels, states with the same symmetry have the same color: red for the s-like ground state, blue for the p-like states, and orange for the d-like states.

TABLE 1: Parameters used in the mobility calculations. Calculated overlap integrals (t), miniband widths (W), and effective masses at Γ (m_x^* and m_y^* are obtained along x and y by fitting the miniband curvature around $q = 0$ with a parabola, according to equation (22). As they are anisotropic for the systems of interest, their arithmetic average $\langle m_\parallel^* \rangle = (m_x^* + m_y^*)/2$ is used in equation (24)) for films of closely packed (interdot separation $d = 1$ bond length) CdSe and PbSe dots with diameter D. The values for the electron confining potential U_0, the density of defects ρ_{defects}, and the size distribution χ (defined as the size difference between 'defect' and "regular" dots) are also reported.

Material	D (nm)	U_0 (eV)	χ (%)	ρ_{defects} (%)	t (meV)	m_x^*	m_y^*	$\langle m_\parallel^* \rangle$	W (meV)
CdSe (wz)	3.84	3.59	5	1	9.0	0.26	0.45	0.36	78
PbSe	2.52	4.56	9.2	1	20.6	0.16	0.20	0.18	257

for the reader to extrapolate our results to higher densities (≤10%), by simply dividing the values reported here by the desired defect density.

On the other hand, unlike in equation (27) (where the temperature dependence has the form—$T^{-1/2}$—expected for acoustic phonon piezoelectric scattering [18]), there is no temperature dependence in equation (24), as (i) in our model, as in Ref. [9], we assume elastic scattering for the electron; (ii) according to the "independent electron approximation" adopted here (where the interaction of each electron with the impurity [defect CQD] is independent of the other electrons), the scattering rate is independent of the electronic distribution function [14]; (iii) the scattering mechanism considered (fluctuations in the QD size) is formally similar to (ionized) impurity scattering, where the scattering rate is independent of temperature [18]; and (iv) the density of the scattering centers ("defect" CQDs) is clearly temperature independent.

Electron mobility in bulk semiconductor materials is influenced by several factors (doping density, density of defects/impurities, and temperature). It is however reasonable to expect that an even larger number of sources should affect it in colloidal quantum dot arrays, owing to the increased complexity of the system, which includes building blocks of potentially different sizes, shapes, mutual orientations, and surface termination, placed at different distances from one another and within a matrix made of a different material. As stated in the introduction, our model assumes size anisotropy as the main source of disorder in these systems, following the suggestion by Shabaev et al. [9], and therefore, the theoretical treatment presented here focuses exclusively on this aspect, neglecting the influence of the other factors mentioned above. Although this may appear as a strong assumption, owing to its simplicity it has been used as a working hypothesis in previous theoretical works [9, 11]. The other most important single source of scattering has been identified [22] as positional disorder. To our knowledge, however, there are no theoretical works treating lattice disorder in CQD arrays within an atomistic framework. This is due to the fact that, in order to account for positional disorder, the supercell used in the calculation of the electronic structure needs to contain a large fraction of the array (i.e., hundreds of thousands of atoms), leading to prohibitively intensive calculations.

From an a posteriori point of view, knowing that both size and positional disorder are likely to be present in experimental samples [22], we can conclude that, since our model reproduces the experimental mobilities to within a factor of ≤1.5 by considering only the former effect, all other effects, including positional disorder, contribute by at most the same amount.

The role of the capping group is also expected to be important, as specific ligands (or the absence thereof) may introduce trap states that will hinder efficient transport, whereas the passivant length determines the interdot separation. We consider films in which all trap states have been removed either through effective passivation [3–5, 8, 23–27] or doping [10].

We tested our results by carrying out Monte Carlo (MC) calculations of the scattering probabilities, considering trajectories for different values for the initial q-vector of the electron, within a specific miniband, and following energy-conserving scattering processes, for values of the applied electric field $E \leq 10^8$ V/cm, also consistent with standard experimental conditions [6]. We found a strong dependence on the specific value of the initial q-vector. However, the MC results for small values of q and the predictions of equation (24) agree within a few percent in the case of films of InAs CQDs.

As defect (or impurity) scattering is a temperature-independent process, the effect of temperature on the mobility can be included by introducing a thermal population of higher q-vector states within the same miniband (the separation between different minibands is much larger than $k_B T$ at room temperature)

$$\mu(T) = \frac{\sum_i \mu_i f(\in_i, T, E_F) n_i}{\sum_i f(\in_i, T, E_F) n_i}. \quad (28)$$

Here, $f(\in_i, T, E_F)$ is the occupation probability of the i-th energy interval (the width of the miniband is divided into a large number of intervals of equal width, within each of which the energy is constant (within ~ 1 meV) and equal to (the average value) $\in_i$), containing n_i states with (average) energy ε_i and Monte Carlo mobility μ_i, and the sum is performed on all intervals. Our recent results [19] are in very good agreement with experiment [6] and confirm a much weaker temperature dependence than predicted by equation (27), in line with observation [6].

It is worth mentioning that other transport mechanisms have been proposed to occur in CQD films: phonon-assisted (or hopping) conduction [22, 28–32] and direct tunnelling [2, 33–35]. This work focuses on band-like transport instead, aiming to investigate recent claims from several different groups, reporting bulk-like transport in CQD films, and following the observation of record high mobilities in these systems [6–8, 10, 36–38]. Our results (presented both in this work and in Ref. [19]) confirm that band-like transport is indeed possible in CQD films and can explain the high electron mobilities observed recently in high-quality CQD films and their temperature dependence [19], which is, instead, inconsistent with the predictions of the conventional hopping model [22]. Furthermore, the application of this simple but, at the same time, surprisingly accurate approach to 2D dot arrays of different materials, crystal structures, lattice arrangements, surface stoichiometries, and morphologies allowed us [17] to provide general design guidelines to tune the electron mobility in these systems.

The mechanism responsible for charge transport in quantum dot films remains, however, controversial, as, recently, transport by small polaron hopping was shown [39] to exhibit, in some parameter range, the temperature dependence observed experimentally [6, 10] and predicted theoretically [19] for band-like transport.

4. Conclusions

In summary, we have derived an order-of-magnitude-accurate expression for the evaluation of the mobility in CQD films. Such an expression, based on simple assumptions and free from any fitting parameter, underpinned recent studies on structural and temperature dependence of the mobility in CQD films, proving strikingly accurate (and much superior to an alternative formula recently proposed in the literature) in reproducing experiment both qualitatively and quantitatively. It therefore represents an effective and useful tool for the prediction of the transport properties of CQD films, which will provide valuable help optimizing the choice of dot materials and their characteristics for specific device applications.

Data Availability

The paper presents a new theoretical framework for the calculation of the electron mobility in nanocrystal films. All data are included in the manuscript.

Conflicts of Interest

The authors declare that they have no conflicts of interest.

Acknowledgments

M.C. gratefully acknowledges financial support from the Royal Society under the URF scheme and GENIL—Strengthening through Short Visits Ref. GENIL-SSV 2014. F.M.G.C. and S.R.B. were supported by Project ENE2016 80944 R, funded by the Spanish Ministerio de Economía, Industria y Competitividad. F.M.G.C. was also funded by Project mPTIC 5 from Campus de Excelencia Internacional BioTic Granada and a mobility grant from the "José Castillejo" program for young researchers funded by Spanish Ministerio de Educación, Cultura y Deporte.

References

[1] D. V. Talapin and C. B. Murray, *Science*, vol. 310, no. 5745, pp. 86–89, 2005.

[2] D. V. Talapin, J.-S. Lee, M. V. Kovalenko, and E. V. Shevchenko, *Chemical Reviews*, vol. 110, no. 1, pp. 389–458, 2010.

[3] J. Tang, K. W. Kemp, S. Hoogland et al., *Nature Materials*, vol. 10, no. 10, pp. 765–771, 2011.

[4] J. Zhang, J. Gao, E. M. Miller, J. M. Luther, and M. C. Beard, "Diffusion-controlled synthesis of PbS and PbSe quantum dots with in situ halide passivation for quantum dot solar cells," *ACS Nano*, vol. 8, no. 1, pp. 614–622, 2014.

[5] C.-H. M. Chuang, P. R. Brown, V. Bulović, and M. G. Bawendi, "Improved performance and stability in quantum dot solar cells through band alignment engineering," *Nature Materials*, vol. 13, no. 8, pp. 796–801, 2014.

[6] J.-S. Lee, M. V. Kovalenko, J. Huang, D. S. Chung, and D. V. Talapin, "Band-like transport, high electron mobility and high photoconductivity in all-inorganic nanocrystal arrays," *Nature Nanotechnology*, vol. 6, no. 6, pp. 348–352, 2011.

[7] S. J. Oh, N. E. Berry, J.-H. Choi et al., "Stoichiometric control of lead chalcogenide nanocrystal solids to enhance their electronic and optoelectronic device performance," *ACS Nano*, vol. 7, no. 3, pp. 2413–2421, 2013.

[8] S. J. Oh, Z. Wang, N. E. Berry et al., "Engineering charge injection and charge transport for high performance PbSe nanocrystal thin film devices and circuits," *Nano Letters*, vol. 14, no. 11, pp. 6210–6216, 2014.

[9] A. Shabaev, A. L. Efros, and A. L. Efros, "Dark and photo-conductivity in ordered array of nanocrystals," *Nano Letters*, vol. 13, no. 11, pp. 5454–5461, 2013.

[10] J.-H. Choi, A. T. Fafarman, S. J. Oh et al., "Bandlike transport in strongly coupled and doped quantum dots: a route to high-performance thin-film electronics," *Nano Letters*, vol. 12, no. 5, pp. 2631–2638, 2012.

[11] C. Delerue, "From semiconductor nanocrystals to artificial solids with dimensionality below two," *Physical Chemistry Chemical Physics*, vol. 16, no. 47, pp. 25734–25740, 2014.

[12] L.-W. Wang and A. Zunger, "Pseudopotential calculations of nanoscale CdSe quantum dots," *Physical Review B*, vol. 53, no. 15, pp. 9579–9582, 1996.

[13] J. C. Slater and G. F. Koster, "Simplified LCAO method for the periodic potential problem," *Physics Review*, vol. 94, no. 6, pp. 1498–1524, 1954.

[14] N. W. Ashcroft and N. Mermin, *Solid State Physics, Holt Rinehart and Winston*, New York, London, 1976.

[15] L. D. Landau and E. M. Lifshitz, *Quantum Mechanics*, Addison-Wesley, Reading Mass, 1965, Eq. (43.1).

[16] E. Conwell and V. F. Weisskopf, *Physics Review*, vol. 77, no. 3, pp. 388–390, 1950.

[17] F. M. Gómez-Campos, S. Rodríguez-Bolívar, and M. Califano, "High-mobility toolkit for quantum dot films," *ACS Photonics*, vol. 3, no. 11, pp. 2059–2067, 2016.

[18] P. Y. Yu and M. Cardona, *Fundamentals of Semiconductors: Physics and Materials Properties*, Springer, Berlin, Heidelberg, 4th edition, 2010.

[19] F. M. Gómez-Campos, S. Rodríguez-Bolívar, E. S. Skibinsky-Gitlin, and M. Califano, "Efficient, non-stochastic, Monte-Carlo-like-accurate method for the calculation of the temperature-dependent mobility in nanocrystal films," *Nanoscale*, vol. 10, no. 20, pp. 9679–9690, 2018.

[20] J. M. An, A. Franceschetti, S. V. Dudiy, and A. Zunger, "The peculiar electronic structure of PbSe quantum dots," *Nano Letters*, vol. 6, pp. 2728–2735, 2006.

[21] J. Jasieniak, M. Califano, and S. E. Watkins, "Size-dependent valence and conduction band-edge energies of semiconductor nanocrystals," *ACS Nano*, vol. 5, no. 7, pp. 5888–5902, 2011.

[22] P. Guyot-Sionnest, "Electrical transport in colloidal quantum dot films," *The Journal of Physical Chemistry Letters*, vol. 3, no. 9, pp. 1169–1175, 2012.

[23] A. H. Ip, S. M. Thon, S. Hoogland et al., "Hybrid passivated colloidal quantum dot solids," *Nature Nanotechnology*, vol. 7, no. 9, pp. 577–582, 2012.

[24] Z. Ning, O. Voznyy, J. Pan et al., "Air-stable n-type colloidal quantum dot solids," *Nature Materials*, vol. 13, no. 8, pp. 822–828, 2014.

[25] J. Y. Woo, J. H. Ko, J. H. Song et al., "Ultrastable PbSe nanocrystal quantum dots via *in situ* formation of atomically thin halide adlayers on PbSe(100)," *Journal of the American Chemical Society*, vol. 136, no. 25, pp. 8883–8886, 2014.

[26] D. B. Straus, E. D. Goodwin, E. A. Gaulding, S. Muramoto, C. B. Murray, and C. R. Kagan, "Increased carrier mobility and lifetime in CdSe quantum dot thin films through surface trap passivation and doping," *Journal of Physical Chemistry Letters*, vol. 6, no. 22, pp. 4605–4609, 2015.

[27] Y. Liu, M. Gibbs, J. Puthussery et al., "Dependence of carrier mobility on nanocrystal size and ligand length in PbSe nanocrystal solids," *Nano Letters*, vol. 10, no. 5, pp. 1960–1969, 2010.

[28] R. E. Chandler, A. J. Houtepen, J. Nelson, and D. Vanmaekelbergh, "Electron transport in quantum dot solids: Monte Carlo simulations of the effects of shell filling, Coulomb repulsions, and site disorder," *Physical Review B*, vol. 75, no. 8, article 085325, 2007.

[29] D. Yu, C. Wang, B. L. Wehrenberg, and P. Guyot-Sionnest, "Variable range hopping conduction in semiconductor nanocrystal solids," *Physical Review Letters*, vol. 92, no. 21, article 216802, 2004.

[30] H. Liu, A. Pourret, and P. Guyot-Sionnest, "Mott and Efros-Shklovskii variable range hopping in CdSe quantum dots films," *ACS Nano*, vol. 4, no. 9, pp. 5211–5216, 2010.

[31] I.-H. Chu, M. Radulaski, N. Vukmirovic, H.-P. Cheng, and L.-W. Wang, "Charge transport in a quantum dot supercrystal," *The Journal of Physical Chemistry C*, vol. 115, no. 43, pp. 21409–21415, 2011.

[32] T. S. Mentzel, V. J. Porter, S. Geyer, K. MacLean, M. G. Bawendi, and M. A. Kastner, "Charge transport in PbSe nanocrystal arrays," *Physical Review B*, vol. 77, no. 7, article 075316, 2008.

[33] D. Yu, C. Wang, and P. Guyot-Sionnest, "*n*-Type conducting CdSe nanocrystal s," *Science*, vol. 300, no. 5623, pp. 1277–1280, 2003.

[34] D. Vanmaekelbergh and P. Liljeroth, "Electron-conducting quantum dot solids: novel materials based on colloidal semiconductor nanocrystals," *Chemical Society Reviews*, vol. 34, no. 4, pp. 299–312, 2005.

[35] M. V. Kovalenko, M. Scheele, and D. V. Talapin, "Colloidal nanocrystals with molecular metal chalcogenide surface ligands," *Science*, vol. 324, no. 5933, pp. 1417–1420, 2009.

[36] T. S. Mentzel, D. D. Wanger, N. Ray et al., "Nanopatterned electrically conductive films of semiconductor nanocrystals," *Nano Letters*, vol. 12, no. 8, pp. 4404–4408, 2012.

[37] E. Talgorn, Y. Gao, M. Aerts et al., "Unity quantum yield of photogenerated charges and band-like transport in quantum-dot solids," *Nature Nanotechnology*, vol. 6, no. 11, pp. 733–739, 2011.

[38] Y. Yang, Z. Liu, and T. Lian, "Bulk transport and interfacial transfer dynamics of photogenerated carriers in CdSe quantum dot solid electrodes," *Nano Letters*, vol. 13, no. 8, pp. 3678–3683, 2013.

[39] N. Prodanovic, N. Vukmirovic, Z. Ikonic, P. Harrison, and D. Indjin, "Importance of polaronic effects for charge transport in CdSe quantum dot solids," *Journal of Physical Chemistry Letters*, vol. 5, no. 8, pp. 1335–1340, 2014.